Electronic Supplementary Material (ESI) for RSC Advances.

Supporting Information

A comparative study of photovoltaic performance between non-fullerene and fullerene based organic solar cells

Bo Jiang,[a] Xin Zhang,[a] Yuanhui Zheng,[b] Gui Yu,[b] Jiannian Yao[a], and Chuanlang Zhan*[a]

Beijing National Laboratory for Molecular Sciences

[a] CAS Key Laboratory of Photochemistry, Institute of Chemistry, Chinese Academy of Sciences, Beijing, P. R. China. Fax: +86-10-82616517. E-mail: clzhan@iccas.ac.cn

[b] *CAS Key Laboratory of Organic Solids, ICCAS, Beijing, P. R. China*

Contents

1. Experimental Section

1.1. Methods

All reagents and chemicals were purchased from commercial sources (TCI, Acros, Sigma, or Alfa) and used without further purification except statements. Solvents (toluene and tetrahydrofuran) were distilled by standard procedures before used for organic synthesis.

^{1}H NMR and ^{13}C NMR spectrums were recorded by a Bruker DMX-400 spectrometer with $CDCl_3$ as a solvent and tetramethylsilane as an internal reference. MALDI-TOF mass spectra were recorded by a Bruker BIFLEXIII. Elemental analysis was performed on a flash EA1112 analyzer.

The cyclic voltammetry (CV) was performed using a Zahner IM6e electrochemical workstation in a 0.1 mol/L tetrabutylammoniumhexafluorophosphate (Bu_4NPF_6) dichloromethane (DCM) solution with a scan speed at 0.1 V/s. A Pt wire and Ag/AgCl were used as the counter and reference electrodes, respectively. The concentration of **Bis-PDI-T-BuO** is 1×10^{-4} mol/L in chromatographic pure DCM for the measurements of CV.

The absorption and emission spectrum were measured on Hitachi U-3010 UV-vis spectrophotometer and Horiba Fluoro Max-4-NIR spectrophotometers, respectively. The pristine films used for the absorption and fluorescence spectrum measurements were prepared by spin-coating a 10 mg/mL chloroform (for PDI dimer) or *o*-DCB (for PBDTTT-C-T and PBDT-TS1) solution on the quartz plates. The blended films used for the absorption and fluorescence spectrum measurements were prepared on the quartz glass substrates under the same conditions (e.g. D/A ratio, spin-coating speed, solvent) as those for preparation of optimal photovoltaic devices. The thickness of the solid films was measured by Dektak Profilometer. The pure film of dimer was prepared from chloroform solution with a concentration of 10 mg/mL because perfect film may be formed using chloroform as the processing solvent.

Transmission electron microscopy (TEM) tests were performed on a JEM-2011F operated at 200 kV. The TEM specimens were prepared by transferring the spin-coated films to the 200 mesh copper grids.

1.2. Molecular modelling

Computational details are presented as follows:

Density functional theory calculations were performed with the Gaussian 09 program, [1] using the B3LYP functional. [2] All-electron double-ξ valence basis sets with polarization functions 6-31G* were used for all atoms. [3] Geometry optimizations were performed with full relaxation of all atoms in gas phase without solvent effects.

1.3. Fabrications and Characterizations of OTFT Devices

An n-type heavily doped Si wafer with a SiO_2 layer of 300 nm (with a capacitance of 11 $nF \cdot cm^{-2}$) served as the bottom gate electrode and dielectric layer, respectively. The bottom Au contacts were prepared by photolithography and the device channel lengths, defined as the distance between source and drain was 5 μm. The channel width was 1400 μm. Before deposition of the organic semiconductor, the gate dielectrics were treated with octadecyltrichlorosilane (OTS) in a vacuum oven at a temperature of 120 °C, forming an OTS self-assembled monolayer. The treated substrates were rinsed successively with hexane, ethanol, and chloroform. A PDI dimer layer was deposited on the OTS-treated Si/SiO_2 substrates by spin-coating of a chlorobenzene (CB) solution (10 mg/ml). The resulting thin films were annealed at 160 °C for 60 minutes in vacuum to dry the solvent and improve the film quality and morphology. The field-effect mobility was calculated in the saturation region using the following equation: $I_{ds}=(WC_i/2L)\mu(V_G-V_T)^2$, where I_{ds} is the drain-source current, W and L are the channel width (1400 μm) and length (5 μm), respectively, μ is the field-effect mobility, C_i is the capacitance per unit area of the insulation layer (SiO_2, 11 $nF \cdot cm^{-2}$), V_G and V_T are the gate and threshold voltages, respectively.

1.4. Fabrication and characterizations of OSCs

OSCs with a conventional configuration of ITO/PEDOT:PSS/polymer:PDI dimer/Ca/Al was fabricated as follows. The ITO glass was pre-cleaned with deionized water, CMOS grade acetone and isopropanol in turn for 15 min. The organic residues were further removed by treating with UV-ozone for 1 h. Then the ITO glass was modified by spin-coating PEDOT:PSS (poly(3,4-ethylenedioxythiophene)-poly(styrenesulfonate) layer, 30 nm) on it. After the ITO glasses were dried in oven at 150 °C for 15 min, the active layer was spin-coated on the PEDOT:PSS using a blend solution of PDI dimer and polymer (30 mg/mL in *o*-dichlorobenzene (*o*-DCB), variants with donor/acceptor weight ratio, and different contents of DIO, respectively), before spin-coating, the blend solutions were stirred at 65°C for 5 hours to dissolve thoroughly. After spin-coating, 7.5 μl *o*-DCB was added in the peri-dish to solvent anneal for 1 h.[4] Ca (20 nm) and Al (80 nm) electrode was then subsequently thermally evaporated on the active layer under the vacuum of 1×10^{-5} Torr. The active area of the device was 0.06 cm^2, and the thicknesses of the active films were ~100 nm. The current-voltage characteristics of all solar cell devices were measured with a Keithley 2400 source and conducted in a nitrogen-filling glove-box. An AM 1.5G solar simulator (AAA grade, XES-70S1) was used as the light source. The light intensity of the solar simulator is calibrated to be 100 mW/cm^2 (at the position of sample) with a standard silicon reference solar cell (Area 20×20 mm^2, the certification of the reference cell is accredited by NIST to the ISO-17025 standard). For light intensity dependence measurements, the incident light power range from 20 to 100 mW/cm^2 through a series of neutral density filters (metallic UV-VIS-NIR, Andover). EQE measurements were determined using an ORIEL IQE 200 (Newport) with a scan rate of 20 nm per point under ambient condition.

1.5. Measurements of the electron mobility by the space-charge limited current (SCLC) method

The devices were fabricated with a configuration of ITO/ZnO (30 nm)/polymer:PDI dimer (~100 nm)/Ca (20 nm)/Al (80 nm). The blended films were prepared using the same condition as the preparation of the best OSC device. Finally, the Ca and Al layer was thermally deposited on the top of the blended films in vacuum. The electron mobilities were extracted by fitting the current density–voltage curves using the following equation (1): [5]

$$JL^3V^2 = 9\varepsilon\varepsilon_0\mu_0/8 \qquad (1)$$

where ε is the dielectric constant of the acceptor material, $\varepsilon_0 = 8.85419\times10^{-12}$ C V^{-1} m^{-1}, μ_e the zero-field mobility, L the thickness of the films, and $V = V_{appl} - V_{bi}$; V_{appl} the applied potential, and V_{bi} the built-in potential which results from the difference in the work function of the anode and the cathode. The results are plotted as ln(*J*) *vs*. ln(*V*) and the electron mobility of the blending films was deduced from the intercept value.

1.6. Measurements of the hole mobility by the space-charge limited current (SCLC) method

The devices were fabricated with configuration of ITO/PEDOT:PSS (30 nm)/polymer:PDI dimer (~100 nm)/Au (80 nm). The Au layer was deposited under a low speed (1 Å/10 s) to avoid the penetration of Au atoms into the active layer. The active layers were spin-coated as the OSCs. The hole mobility was extracted by fitting the current density–voltage curves using the equation (1). The results are plotted as ln(*J*) *vs*. ln(*V*) and the hole mobility of the blending films was deduced from the intercept value.

2. Synthesis and Characterization

1-(n-butoxyl)-7-brominated PDI (monomer 1) were synthesized following our reported procedure. [6,7]

Synthesis of Bis-PDI-T-BuO

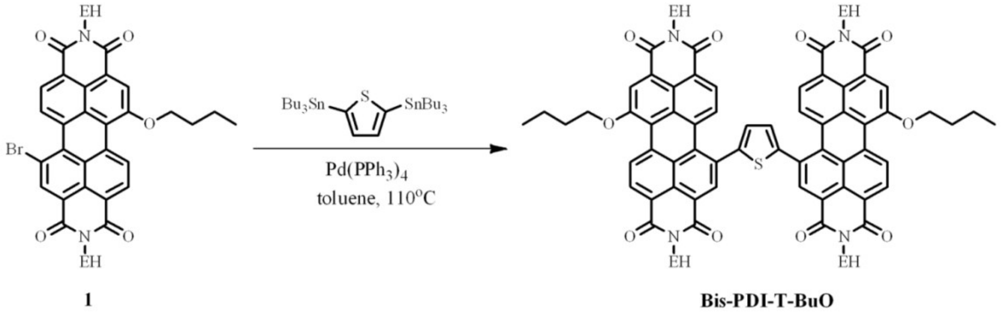

A mixture of 1 (168.5 mg, 0.22 mmol) and 2,5-bis(tributylstannyl) thiophene (97%, 0.1mmol) was dissolved in dry toluene (10 mL). Catalytic amounts of $Pd[P(C_6H_5)_3]_4$ was added and the reaction mixture was stirred at 110 °C for 36 hours. The mixture was extracted with dichloromethane (DCM), washed with water. Then, DCM layer was dried over Na_2SO_4. After removal of DCM, the residue was applied to chromatography with CH_2Cl_2/ethanol (100:1) as eluents to afford the desired products **O2** only as a black solid (115.0 mg, 0.081 mmol, yield = 81%).

^{1}H-NMR (400MHz, $CDCl_3$) δ ppm: 9.42-8.24 (m, 12H), 7.46 (s, 2H), 4.51 (m, 4H), 4.25-3.98 (m, 8H), 2.06 (m, 4H), 2.03-1.82 (m, 4H), 1.65 (m, 4H), 1.50-1.16 (m, 32H), 1.08 (m, 6H), 1.04-0.76 (m, 24H). ^{13}C-NMR (100 MHz, $CDCl_3$) δ ppm: 163.8, 163.5, 163.5, 156.9, 144.0, 139.1, 134.3, 133.5, 133.2, 131.7, 129.4, 128.8, 128.6, 127.9, 125.7, 124.0, 123.6, 122.1, 121.7, 121.5, 120.8, 57.6, 51.2, 44.5, 41.3, 38.0, 31.0, 28.9, 24.3, 23.6, 23.2, 14.3, 10.8.MS (MALDI-TOF): *m/z* = 1454.7 $[M+H]^+$. Elemental analysis: calcd (%) for $C_{92}H_{100}N_4O_{10}S$: C 76.00, H 6.93, N 3.85, S 2.21; found C 75.63, H 6.95, N 3.86, S 2.21.

3. Supporting Figures

Fig. S1 The optimal conformations of the PDI dimer **Bis-PDI-T-BuO** and the dihedral angles are shown in the following table.

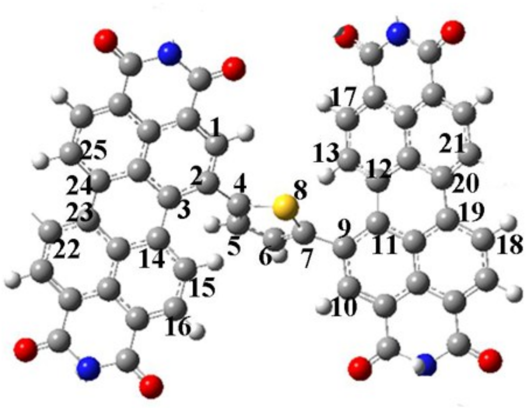

Atom Number	1-2-4-5	1-2-4-8	3-2-4-5	3-2-4-8
θ(°)	-125.45	49.59	50.03	-134.93
Plane	perylene-thiophene	perylene-thiophene	perylene-thiophene	perylene-thiophene
Atom Number	10-9-7-8	10-9-7-6	11-9-7-8	11-9-7-6
θ(°)	119.94	-53.58	-56.10	130.39
Plane	perylene-thiophene	perylene-thiophene	perylene-thiophene	perylene-thiophene
Atom Number	9-11-12-13	18-19-20-21	2-3-14-15	22-23-24-25
θ(°)	-20.59	-15.30	21.01	14.80
Plane	naphthalene-naphthalene	naphthalene-naphthalene	naphthalene-naphthalene	naphthalene-naphthalene
Atom Number	15-16-13-17	1-2-9-10		
θ(°)	-19.08	164.02		
Plane	perylene-perylene	perylene-perylene		

Fig. S2 Cyclic voltammogram (CV) of **Bis-PDI-T-BuO** in a 0.1 mol L^{-1} Bu_4NPF_6/CH_2Cl_2 solution with a scan rate of 50 mV s^{-1}.

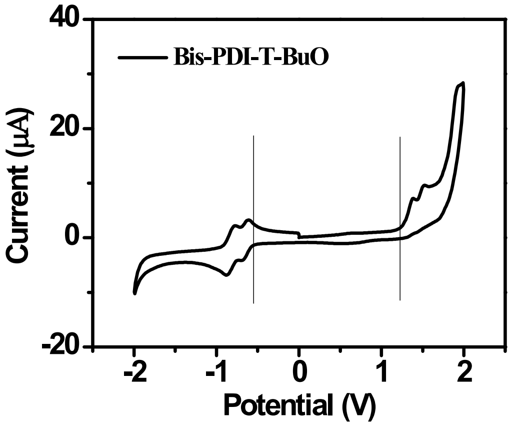

Fig. S3 Energy level alignments of the components in the conventional device based on PBDTTT-C-T.

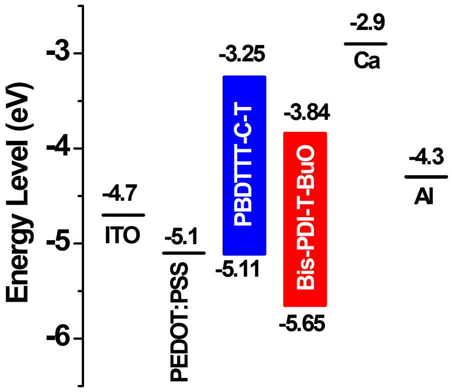

Fig. S4 Plots of ln(J) vs. ln(V) obtained from the electron-only (A) and hole-only (B) devices based on PBDTTT-C-T/Bis-PDI-T-BuO, respectively, which were estimated using the SCLC method.

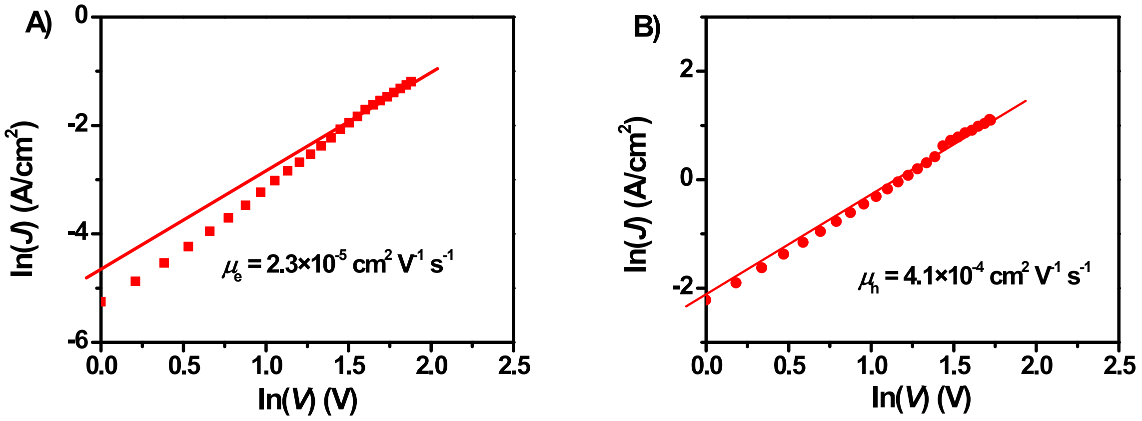

Fig. S5 Plots of ln(J) vs. ln(V) obtained from the electron-only (A) and hole-only (B) devices based on PBDTTT-C-T/PC$_{71}$BM, respectively, which were estimated using the SCLC method.

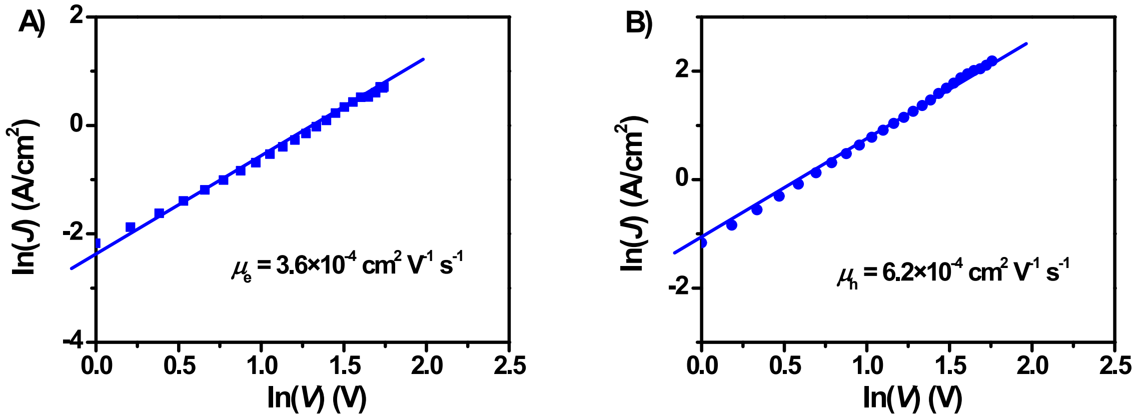

Fig. S6 UV-vis absorption spectra of Bis-PDI-T-BuO, PBDTTT-C-T and PBDT-TS1 in thin film, respectively.

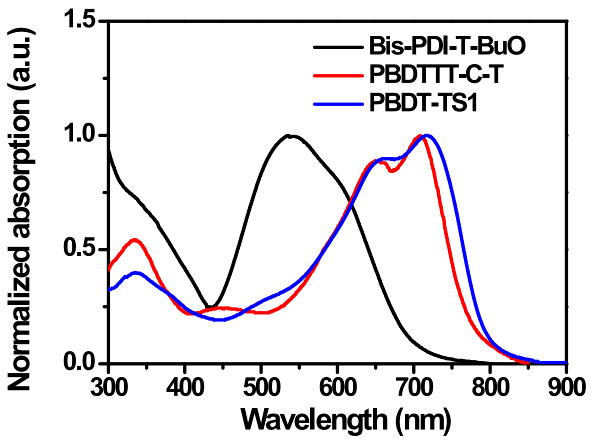

Fig. S7 Energy level alignments of the components in the conventional device based on PBDT-TS1.

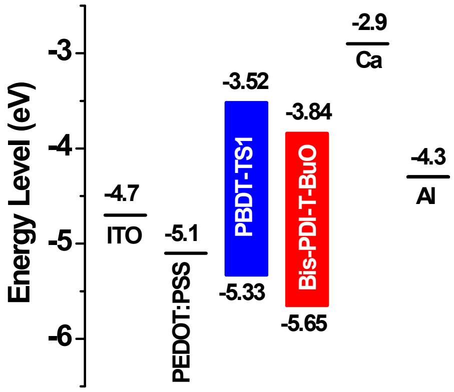

Fig. S8 The *J-V* plots of the optimal devices with PBDT-TS1 as the donor, respectively.

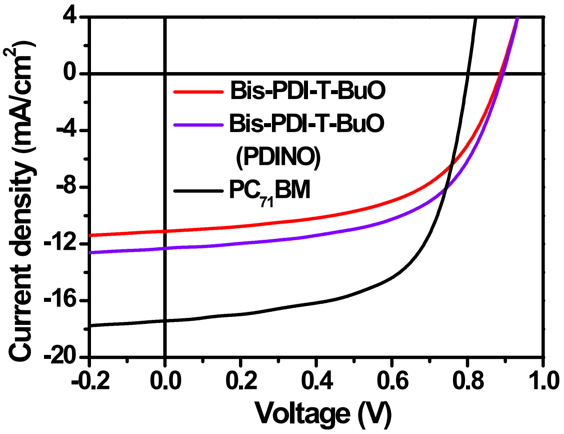

Fig. S9 ^{1}H-NMR spectrum of **Bis-PDI-T-BuO**.

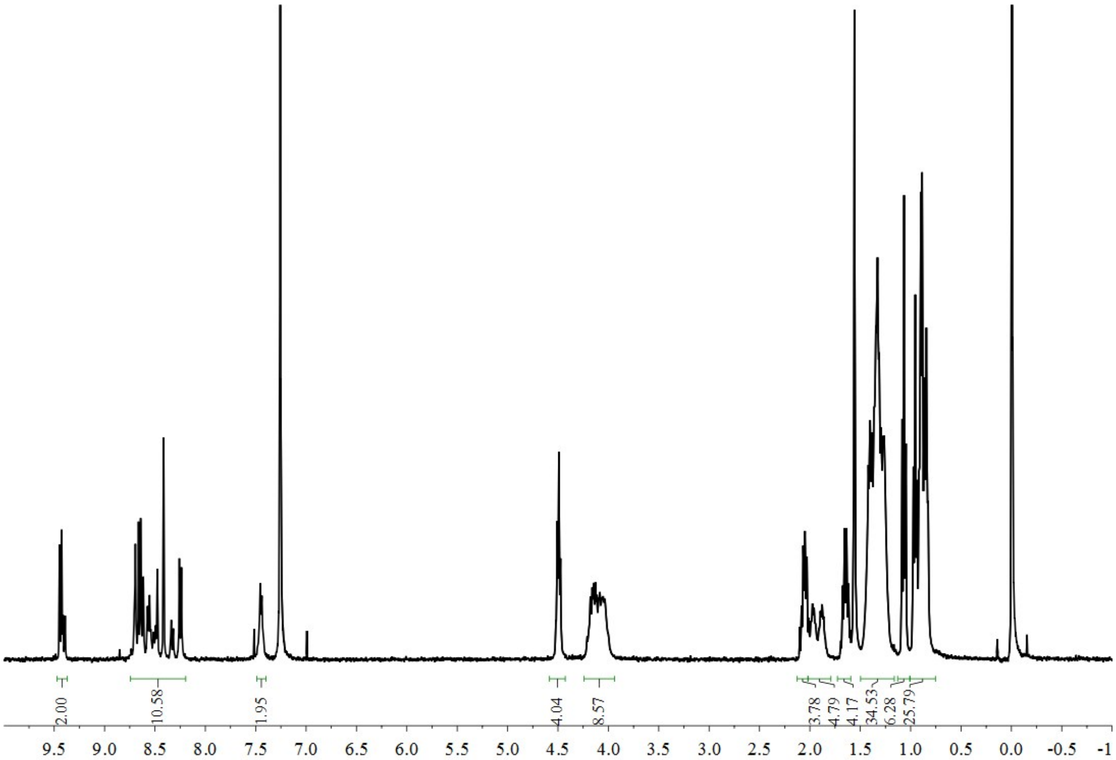

Fig. S10 ^{13}C-NMR spectrum of **Bis-PDI-T-BuO**.

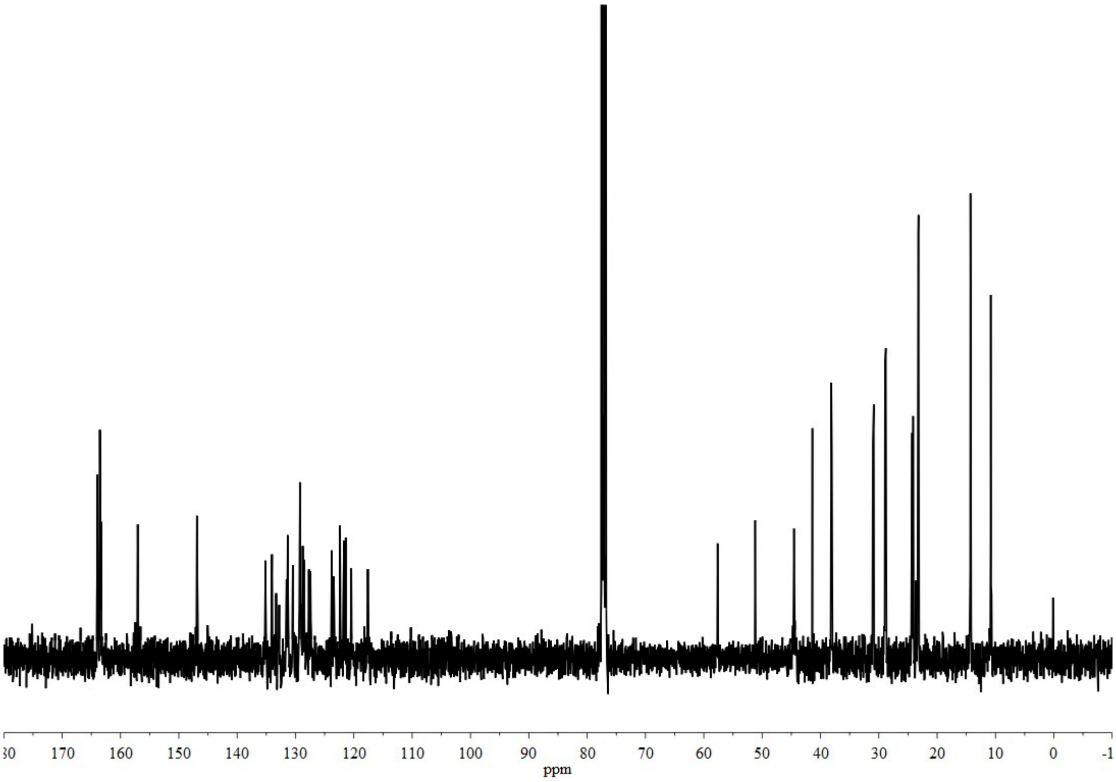

4. Supporting Tables

Table S1. Photovoltaic properties of **PBDTTT-C-T/Bis-PDI-T-BuO** based conventional OSCs.[a]

D/A	DIO	V_{oc}	J_{sc}	J_{cal}[b]	FF	PCE (%)	
	(%, v/v)	(V)	(mA/cm^2)	(mA/cm^2)	(%)	best	ave.[c]
1:1.5	0	0.87	2.24	-	32.4	0.63	0.55
1.5:1	0	0.72	1.27	-	38.3	0.35	0.31
1:1	0	0.84	3.00	-	31.7	0.80	0.73
1:1	1	0.85	8.54	-	54.7	3.97	3.91
1:1	2	0.86	8.53	8.22	59.5	4.36	4.20
1:1	2[b]	0.83	11.04	10.85	57.02	5.24	5.12
1:1	3	0.85	7.60	-	58.6	3.78	3.66
1:1	4	0.85	6.96	-	59.7	3.65	3.52

[a] Tested under AM 1.5G illumination of 100 mW/cm^2. [b] Solvent-vapor annealing was conducted by pre-adding 7.5 µl of *o*-DCB in a lid-fully-covering petri dish before the deposition of the wet photoactive layer atop the ITO/PEDOT:PSS substrate. The annealing time is 8 h. [c] Current densities calculated from the integration of the EQE curves. [c] Average values from 10 devices.

Table S2. Photovoltaic properties of **PBDT-TS1/Bis-PDI-T-BuO** based conventional OSCs.[a]

D/A	DIO	V_{oc}	J_{sc}	FF	PCE (%)	
	(%, v/v)	(V)	(mA/cm^2)	(%)	best	ave.[d]
1:1	3	0.89	10.58	42.29	3.97	3.68
1:2	3	0.93	7.38	51.26	3.50	3.32
1:1.5	1	0.92	11.65	42.53	4.58	4.26
1:1.5	2	0.89	11.44	47.56	4.82	4.57
1:1.5	3	0.89	10.73	51.03	4.85	4.63
1:1.5	3[b]	0.89	11.11	55.99	5.50	5.36
1:1.5	3[b,c]	0.89	12.28	58.17	6.36	6.18
1:1.5	4	0.89	9.94	50.05	4.41	4.28

[a] Tested under AM 1.5G illumination of 100 mW/cm^2. [b] Solvent-vapor annealing was conducted by pre-adding 7.5 µl of *o*-DCB in a lid-fully-covering petri dish before the deposition of the wet photoactive layer atop the ITO/PEDOT:PSS substrate. The annealing time is 1 h. [c] PDINO was used as electron extraction layer to replace Ca. [d] Average values from 10 devices.

5. References

[1] M. J. Frisch, G. W. Trucks, H. B. Schlegel, G. E. Scuseria,M. A. Robb, J. R. Cheeseman, G. Scalmani, V. Barone, B. Mennucci, G. A. Petersson, H. Nakatsuji, M. Caricato, X. Li, H. P. Hratchian, A. F. Izmaylov, J. Bloino, G. Zheng, J. L. Sonnenberg, M. Hada, M. Ehara, K. Toyota, R. Fukuda, J. Hasegawa, M. Ishida, T. Nakajima, Y. Honda, O. Kitao, H. Nakai, T. Vreven, J. A. Montgomery, Jr., J. E. Peralta, F. Ogliaro, M. Bearpark, J. J. Heyd, E. Brothers, K. N. Kudin, V. N. Staroverov, R. Kobayashi, J. Normand, K. Raghavachari, A. Rendell, J. C. Burant, S. S. Iyengar, J. Tomasi, M. Cossi, N. Rega, J. M. Millam, M. Klene, J. E. Knox, J. B. Cross, V. Bakken, C. Adamo, J. Jaramillo, R. Gomperts, R. E. Stratmann, O. Yazyev, A. J. Austin, R. Cammi, C. Pomelli, J. W. Ochterski, R. L. Martin, K. Morokuma, V. G. Zakrzewski, G. A. Voth, P. Salvador, J. J. Dannenberg, S. Dapprich, A. D. Daniels, O. Farkas, J. B. Foresman, J. V. Ortiz, J. Cioslowski, and D. J. Fox, Gaussian 09, Revision A.02, Gaussian, Inc., Wallingford CT, 2009.

[2] a) C. T. Lee, W. T. Yang, R. G. Parr, *Phys. Rev. B* 1988, **37**, 785–789; b) A. D. Becke, *J. Chem. Phys.* 1993, **98**, 5648–5652.

[3] R. Krishnan, J. S. Binkley, R. Seeger, J. A. Pople, *J. Chem. Phys.* 1980, **72**, 650–654.

[4] X. Zhang, C. Zhan, J. Yao, *Chem. Mater.* 2014, DOI: 10.1021/cm504140c.

[5] G. G. Malliaras, J. R. Salem, P. J. Brock, C. Scott, *Phys. Rev. B* 1998, **58**, 13411–13414.

[6] X. Zhang, S. F. Pang, Z. G. Zhang, X. L. Ding, S. L. Zhang, S. G. He, C. L. Zhan, *Tetrahedron Lett.* 2012, **53**, 1094–1097.

[7] X. Zhang, Z. Lu, L. Ye, C. Zhan, J. Hou, S. Zhang, B. Jiang, Y. Zhao, J. Huang, S. Zhang, Y. Liu, Q. Shi, Y. Liu, J. Yao, *Adv. Mater*. 2013, **25**, 5791–5797.